Quantitative Analysis of RIS-Assisted NOMA Systems: BER, Outage Probability, and Ergodic Capacity in $\kappa - \mu$ Fading Channels

Said Awad[1], Mohammed Abdel-Hafez[2]

United Arab Emirates University, Department of Electrical and Communication Engineering, Al-Ain, United Arab Emirates e-mail:[1]201990104@uaeu.ac.ae, [2]mhafez@uaeu.ac.ae

***Abstract*—This paper presents a comprehensive performance analysis of a two-user Non-Orthogonal Multiple Access (NOMA) system, with and without including Reconfigurable Intelligent Surface (RIS) elements, over $\kappa - \mu$ fading channels. The analysis focuses on key performance metrics, including Bit Error Rate (BER), Outage Probability, and Ergodic Capacity, under perfect and imperfect Successive Interference Cancellation (SIC). Integrating RIS in NOMA systems significantly enhances system performance, particularly in mitigating interference and improving signal quality for both near and far users. Analytical results are validated through Monte Carlo simulations for the case when $\kappa = 1$ and $\mu = 1$ to prove that the introduction of the RIS elements into the NOMA system will improve the overall system performance in terms of BER, Outage Probability, and Ergodic Capacity thereby making the system more robust and resilient to the practical scenarios.**

Keywords— Reconfigurable Intelligent Surfaces, Cooperative NOMA, Outage probability, BER, Ergodic Capacity, Imperfect SIC, $\kappa - \mu$ Fading Channels.

I. Introduction

The advent of fifth-generation (5G) and beyond wireless communication systems has ushered in an era of high demand for data rates, energy efficiency, and massive device connectivity. As the world prepares for the deployment of these advanced communication networks, traditional Orthogonal Multiple Access (OMA) techniques are increasingly seen as inadequate to meet the rising demands. Consequently, Non-Orthogonal Multiple Access (NOMA) has emerged as a promising solution, enhancing spectral efficiency by allowing multiple users to share the same time and frequency resources. This is accomplished by superposition coding at the transmitter and successive interference cancellation (SIC) at the receiver[1, 2]. NOMA's ability to offer superior performance in terms of spectral efficiency, reduced latency, and support for massive connectivity has established it as a key technology for next-generation wireless networks [3].

Simultaneously, Reconfigurable Intelligent Surfaces (RIS) have garnered significant attention for their potential to improve wireless communication by controlling the propagation of electromagnetic waves in a cost-effective manner. RIS technology consists of passive reflecting elements that can be dynamically reprogrammed to optimize signal reflection, thereby improving coverage, energy efficiency, and spectral efficiency [4]. Unlike traditional relaying techniques, which require active components and power consumption, RIS can enhance the communication environment without additional energy use, making it a highly scalable and energy-efficient solution for future networks [5]. With its ability to establish virtual line-of-sight (LoS) links, RIS can effectively mitigate the effects of fading, shadowing, and other impairments, particularly in urban and dense environments [6].

The integration of RIS and NOMA is a subject of active research due to its potential to address critical communication challenges. Compared to traditional OMA schemes, RIS-assisted NOMA systems have been shown to significantly improve outage probability, ergodic capacity, and energy efficiency [7]. By leveraging RIS's ability to manipulate the wireless environment and NOMA's spectral advantages, these systems are particularly beneficial for cell-edge users who typically suffer from poor signal quality. Deploying RIS strategically in urban infrastructure can extend coverage and improve communication quality [4, 5].

Recent research highlights the importance of considering practical scenarios, such as imperfect SIC and hardware impairments, in analyzing RIS-assisted NOMA networks. Imperfect SIC, where the residual interference impacts system performance, has been studied to understand its effect on outage probability and Bit Error Rate (BER) [6, 8]. Furthermore, studies on the ergodic performance of RIS-NOMA systems under realistic fading conditions, such as $\kappa - \mu$ channels, underscore the robustness and adaptability of this technology [3, 7]. Applications of RIS extend beyond simple reflections; they can be integrated into various surfaces, from building facades to vehicle exteriors, offering scalable solutions for diverse deployment scenarios [4, 9].

This work performs a comprehensive analysis of two-user NOMA systems with and without RIS elements over $\kappa - \mu$ fading channels. We analyze key performance metrics—BER, Outage Probability, and Ergodic Capacity—under perfect and imperfect SIC conditions. The analytical results, validated through Monte Carlo simulations, reveal that integrating RIS elements can significantly enhance system performance, making it more robust and efficient [10]. The study also discusses the impact of power allocation strategies and interference management on overall performance, drawing on findings from

979-8-3315-2096-0/25/$31.00 ©2025 IEEE

cooperative and cognitive NOMA systems [11, 12].

II. System and Channel Models

In this paper, the main focus is on the performance analysis of a NOMA system in the presence of RIS. First, the analysis of the two-user NOMA downlink system without the presence of RIS elements as shown in Fig. 1. Consider a scenario where we have two users, U1 and U2, such that U1 is a far user and U2 is a near user. Also, let the transmitted symbol be given by $x = \sqrt{P_1}x_1 + \sqrt{P_2}x_2$ where, P_1 and P_2 are the power allocated to user 1 (U1) and user 2 (U2) respectively. As U1 is the far user and U2 is the near user, $P_1 > P_2$.

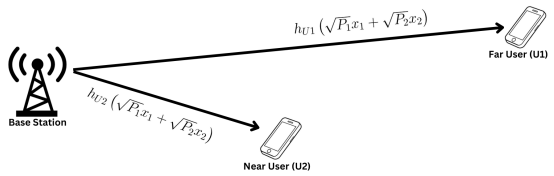

Fig. 1: NOMA System without RIS elements

Similarly, when we use N-RIS elements, as shown in Fig. 2, we get the system model as follows:

$$y_{U1} = h_{U1}x + \sum_{i=0}^{N-1} h_{RIS_i,U1}x + \sigma_{U1}^2 \tag{1}$$

$$y_{U2} = h_{U2}x + \sum_{i=0}^{N-1} h_{RIS_i,U2}x + \sigma_{U2}^2 \tag{2}$$

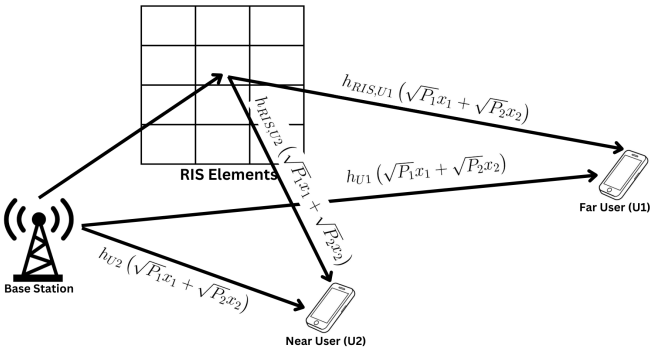

Fig. 2: NOMA System with RIS elements

Consider the case without RIS in which the received signals at U1 and U2 are given, respectively, by $y_{U1} = h_{U1}x + n_{U1}$ and $y_{U2} = h_{U2}x + n_{U2}$ where, h_{U1} and h_{U2} are the channel between the base station (BS) and U1, BS and U2, respectively. n_{U1} and n_{U2} are the AWGN noise at U1 and U2, respectively, with their corresponding variance being σ_{U1} and σ_{U2}. The received signal at U1 and U2 without RIS are given by:

$$y_{U1} = h_{U1}\left(\sqrt{P_1}x_1 + \sqrt{P_2}x_2\right) + n_{U1} \tag{3}$$

$$y_{U2} = h_{U2}\left(\sqrt{P_1}x_1 + \sqrt{P_2}x_2\right) + n_{U2} \tag{4}$$

The U1 just have to decode the message x_1. During the process, it assumes the message signal x_2 as a part of the noise. In contrast, the U2 needs to first decode the message x_1 and remove it from the received signal using the successive interference cancellation (SIC) method and then have to decode the message x_2. In practical systems with imperfect SIC, the symbol x_1 will cause interference in decoding the message signal x_2.

A. Instantaneous SNR without RIS Elements

The instantaneous SNR at U1 for the symbol x_1 and at U2 for the symbol x_2 are given by γ_{U1} and γ_{U2}, respectively, which are given by the expressions:

$$\gamma_{U1} = \frac{P_1|h_{U1}|^2}{P_2|h_{U2}|^2 + \sigma_{U1}^2} \tag{5}$$

$$\gamma_{U2} = \frac{P_2|h_{U2}|^2}{\beta P_1|h_{U2}|^2 + \sigma_{U2}^2} \tag{6}$$

where, $0 < \beta < 1$ denotes the residual interference due to improper SIC.

III. BER Analysis

A. BER Analysis without RIS Elements

As the channel between the BS and users (both U1 and U2) follows a $\kappa - \mu$ fading the *pdf* of the channel for the i^{th} user (Ui) is given by the expression:

$$f_{Ui}(\gamma_{Ui}) = \frac{\mu^{\mu}\left(1+\kappa\right)^{\frac{\mu+1}{2}}\gamma_{Ui}^{\frac{\mu-1}{2}}e^{-\mu(1+\kappa)\gamma_{Ui}}}{\Gamma\left(\mu\right)\kappa^{\frac{\mu-1}{2}}} \times\mathcal{I}_{\mu-1}\left(2\mu\sqrt{\kappa\left(1+\kappa\right)\gamma_{Ui}}\right) \tag{7}$$

where $\mathcal{I}_m(\cdot)$ is the Bessel function of the first kind of the order m. The BER of BPSK modulation for the i^{th} user is given by the expression:

$$BER_{Ui} = \int_0^{\infty} \mathcal{Q}_{\mu}\left(\sqrt{2\gamma_{Ui}}\right) f_{Ui}\left(\gamma_{Ui}\right) d\gamma_{Ui} \tag{8}$$

By using the moment generating function (MGF) approach, the expression for the BER can be approximated as

$$BER_{Ui} = \frac{1}{2}\left[1 - M_{\gamma_{Ui}}\left(\frac{1}{2}\right)\right] \tag{9}$$

where, $M_{\gamma_{Ui}}(s)$ is the MGF for the i^{th} user (Ui) and is derived using the expression $\mathbb{E}\left[e^{-s\gamma_{Ui}}\right]$. For a $\kappa-\mu$ channel the MGF function is given by

$$M_{Ui} = \left(\frac{\Psi_{Ui}\mu(1+\kappa)}{1+\Psi_{Ui}\mu(1+\kappa)}\right)^{\mu} e^{-\mu\kappa\frac{1}{1+\Psi_{Ui}\mu(1+\kappa)}} \tag{10}$$

where, Ψ_{Ui} is the average received SNR at Ui.

1) BER Analysis of User 1 (U1): The BER at U1 is given by the expression

$$BER_{Ui} = \frac{1}{2}\left[1 - M_{\gamma_{Ui}}\left(\frac{1}{2}\right)\right] \tag{11}$$

And the MGF is given by

$$M_{U1} = \left(\frac{\Psi_{Ui}\mu(1+\kappa)}{1+\Psi_{U1}\mu(1+\kappa)}\right)^{\mu} e^{-\mu\kappa\frac{1}{1+\Psi_{U1}\mu(1+\kappa)}} \tag{12}$$

where the average received SNR at U1 is given by $\Psi_{U1} = \mathbb{E}\left\{\frac{P_1|h_{U1}|^2}{P_2|h_{U1}|^2+\sigma_{U1}^2}\right\}$.

2) BER Analysis of User 2 (U2): Based on the NOMA protocol presented above, first, the U2 has to decode x_1, perform SIC to remove it, and then decode x_2. Using the same lines above, we find that the instantaneous SNR of x_1 for U2 is given by $\gamma_{U2,x_1} = \frac{P_1|h_{U2}|^2}{P_2|h_{U2}|^2+\sigma_{U2}^2}$ and the SNR of x_2 for U2 considering the improper SIC is given by $\gamma_{U2,x_2} = \frac{P_2|h_{U2}|^2}{\sigma_{U2}^2+\beta P_1|h_{U2}|^2}$ where, $0 < \beta < 1$ denotes residual interference due to improper SIC as explained above. Hence, the effective BER of U2 is given by the effective sum of BER_{U2,x_1} and BER_{U2,x_2} i.e.., $BER_{U2} = BER_{U2,x_1} + BER_{U2,x_2}$. The effect of using RIS on the system BER performance is discussed next.

B. BER Analysis with N-RIS Elements

The instantaneous SNR for x_1 is given by:

$$\gamma_{U1} = \frac{P_1 \times \left(|h_{U1}|^2 + \sum_{i=0}^{N-1}|h_{RIS_i,U1}|^2\right)}{P_2 \times \left(|h_{U1}|^2 + \sum_{i=0}^{N-1}|h_{RIS_i,U1}|^2\right) + \sigma_{U1}^2} \tag{13}$$

So, we get the average SNR at U1 for x_1 as:

$$\Psi_{U1,x_1,N_{RIS}} = \mathbb{E}\left\{\frac{P_1 \times \left(|h_{U1}|^2 + \sum_{i=0}^{N-1}|h_{RIS_i,U1}|^2\right)}{P_2 \times \left(|h_{U1}|^2 + \sum_{i=0}^{N-1}|h_{RIS_i,U1}|^2\right) + \sigma_{U1}^2}\right\} \tag{14}$$

Similarly, we get $\Psi_{U2,x_1,N_{RIS}}$ and $\Psi_{U2,x_2,N_{RIS}}$ as:

$$\Psi_{U2,x_1,N_{RIS}} = \mathbb{E}\left\{\frac{P_1 \times \left(|h_{U2}|^2 + \sum_{i=0}^{N-1}|h_{RIS_i,U2}|^2\right)}{P_2 \times \left(|h_{U2}|^2 + \sum_{i=0}^{N-1}|h_{RIS_i,U2}|^2\right) + \sigma_{U2}^2}\right\} \tag{15}$$

$$\Psi_{U2,x_2,N_{RIS}} = \mathbb{E}\left\{\frac{P_2 \times \left(|h_{U2}|^2 + \sum_{i=0}^{N-1}|h_{RIS_i,U2}|^2\right)}{\beta \times P_2 \times \left(|h_{U2}|^2 + \sum_{i=0}^{N-1}|h_{RIS_i,U2}|^2\right) + \sigma_{U2}^2}\right\} \tag{16}$$

The MGF and the BER is computed by substituting the values $\Psi_{U1,N_{RIS}}$, $\Psi_{U2,x_1,N_{RIS}}$ and $\Psi_{U2,x_2,N_{RIS}}$ in corresponding equations which are derived above.

IV. Outage Probability Analysis

The outage probability (OP) for the i^{th} user is defined as the probability that the received SNR (instantaneous SNR) γ is less than the threshold $\eta_{th} = 2^{R_{th}}$, where R_{th} denotes the data rate expressed by

$$\mathcal{P}_{out}(\eta_{th}) = \text{Prob}\left(\gamma < \eta_{th}\right) \tag{17}$$

The above expression can be written in terms of *cdf* as $\mathcal{P}_{out}(\eta_{th}) = F_{\gamma}(\eta_{th})$. For the $\kappa-\mu$ channel, the OP is given by the expression

$$F_{\gamma}(x) = 1 - \mathcal{Q}_{\mu}\left(\sqrt{2\kappa\mu}, \sqrt{\frac{2\mu\ (\kappa+1)x}{\Psi}}\right) \tag{18}$$

where $\mathcal{Q}_{\mu}$ is called as the Marcum-Q function, which can be approximated by the infinite series expansion $\mathcal{Q}_{\mu} = \sum_{l=0}^{\infty}\sum_{k=0}^{\mu+l-1}\frac{s^{2l}t^{2k}}{l!k!2^{l+k}}e^{-\frac{s^2+t^2}{2}}$.

A. Outage Probability for User 1 (U1)

The expression the gives the outage probability for the U1

$$\mathcal{P}_{out,U1}(\eta_{th}) = 1 - \mathcal{Q}_{\mu}\left(\sqrt{2\kappa\mu}, \sqrt{\frac{2\mu(\kappa+1)\eta_{th}}{\Psi_{U1}}}\right) \tag{19}$$

B. Outage Probability for User 2 (U2)

The expression that gives the outage probability for the U2

$$\begin{aligned}\mathcal{P}_{out,U2}(\eta_{th}) &= \mathcal{P}_{out,U2,x_1}(\eta_{th}) + \mathcal{P}_{out,U2,x_2}(\eta_{th}) \\ &\quad - \mathcal{P}_{out,U2,x_1}(\eta_{th})\mathcal{P}_{out,U2,x_2}(\eta_{th})\end{aligned} \tag{20}$$

$$\begin{aligned}\mathcal{P}_{out,U2}(\eta_{th}) &= 1 - \mathcal{Q}_{\mu}\left(\sqrt{2\kappa\mu}, \sqrt{\frac{2\mu(\kappa+1)\eta_{th}}{\Psi_{U2,x_1}}}\right) \\ &\quad + 1 - \mathcal{Q}_{\mu}\left(\sqrt{2\kappa\mu}, \sqrt{\frac{2\mu(\kappa+1)\eta_{th}}{\Psi_{U2,x_2}}}\right) \\ &\quad - \left(1 - \mathcal{Q}_{\mu}\left(\sqrt{2\kappa\mu}, \sqrt{\frac{2\mu(\kappa+1)\eta_{th}}{\Psi_{U2,x_1}}}\right)\right) \\ &\quad \times \left(1 - \mathcal{Q}_{\mu}\left(\sqrt{2\kappa\mu}, \sqrt{\frac{2\mu(\kappa+1)\eta_{th}}{\Psi_{U2,x_2}}}\right)\right)\end{aligned} \tag{21}$$

where Ψ_{Ui,x_j}, for $i = 1, 2$ and $j = 1, 2$, are defined earlier for the two scenarios, with and without N-RIS elements.

V. Ergodic Capacity

This section obtains the ergodic capacities (ECs) of U1 and U2. If the received SNR is γ, then the instantaneous capacity is given by the formula

$$\mathcal{C} = \log_2(1+\gamma) \tag{22}$$

The ergodic capacity is obtained by taking the expectation of the instantaneous capacity and is given by the expression

$$\bar{\mathcal{C}} = \frac{1}{\ln 2}\int_0^{\infty}\log_2(1+\gamma)f_{\gamma}(y)dy \tag{23}$$

From [2], it can be observed that we can write the equation (17) as

$$\begin{aligned}\bar{\mathcal{C}} &= \frac{1}{\ln 2}\int_0^{\infty}\frac{1-F_{\gamma}(y)}{1+y}dy \\ &= \frac{1}{2\ln 2}\sum_{r=0}^{\infty}\sum_{j=0}^{\mu+r+1}\frac{\mu^{r+j}}{r!j!}\left(\frac{1+\kappa}{\Psi}\right)^{j}\Gamma(j+1) \\ &\quad \times \Gamma\left(-j, \frac{\mu(1+\kappa)}{\Psi}\right)e^{\mu}\end{aligned} \tag{24}$$

A. Ergodic Capacity for User 1 (U1)

The expression that gives the ergodic capacity of U1 is

$$\begin{aligned}\bar{\mathcal{C}}_{U1} &= \frac{1}{2\ln 2}\int_0^{\infty}\frac{1-F_{\gamma_{U1}}(y)}{1+y}dy \\ &= \frac{1}{2\ln 2}\sum_{r=0}^{\infty}\sum_{j=0}^{\mu+r+1}\frac{\mu^{r+j}}{r!j!}\left(\frac{1+\kappa}{\Psi_{U1}}\right)^{j}\Gamma(j+1) \\ &\times\Gamma\left(-j,\frac{\mu(1+\kappa)}{\Psi_{U1}}\right)e^{\mu}\end{aligned} \tag{25}$$

where Ψ_{Ui}, for $i = 1, 2$, are defined earlier for the two scenarios, with and without N-RIS elements.

B. Ergodic Capacity for User 2 (U2)

Similarly, the ergodic capacity of U2 is given by the expression

$$\bar{\mathcal{C}}_{U2} = \bar{\mathcal{C}}_{U2,x_1} + \bar{\mathcal{C}}_{U2,x_2} \tag{26}$$

the values for the expression $\bar{\mathcal{C}}_{U2,x_1}$ and $\bar{\mathcal{C}}_{U2,x_2}$ can be obtained by using the steps followed above to evaluate that of U1.

VI. Numerical and Simulation Results

This section presents analytical results derived from the previous sections. These analytical results are further verified using Monte Carlo simulations. As specified in the earlier sections, we will consider a system with two users: the far user U1 and the near user U2.

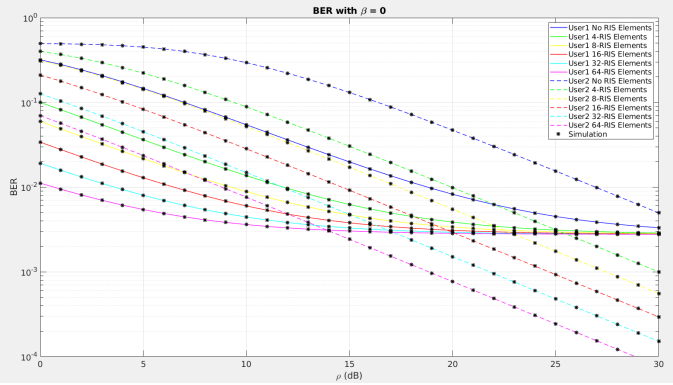

Fig. 3: BER of users U1 and U2 for various RIS scenarios with perfect SIC i.e.., $\beta = 0$ and $P_1 = 0.9$ and $P_2 = 0.1$ and $\kappa = \mu = 1$

Fig. 3 illustrates the BER of users U1 and U2 with perfect Successive Interference Cancellation (SIC), i.e., $\beta = 0$ and $P_1 = 0.9$ and $P_2 = 0.1$, under various scenarios. It can be observed that the BER at U1 saturates, as the signal of U2 is always treated as noise. Since both signals, x_1 and x_2, experience the same channel conditions, the SNR at U1 asymptotically approaches $\frac{P_1}{P_2}$. It can be observed from the figure that the performance of the system increases with the introduction/ increase of RIS elements. Fig. 4 will illustrate the scenario with an imperfect SIC at the U2 with a factor of $\beta = 0.01$. The imperfect SIC will depreciate the U2

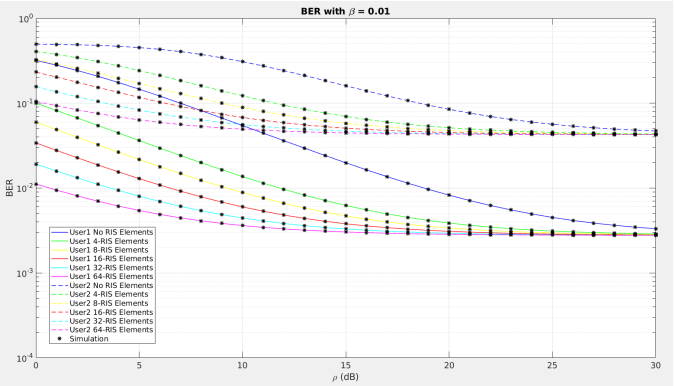

Fig. 4: BER of users U1 and U2 for various RIS scenarios with imperfect SIC i.e.., $\beta = 0.01$ and $P_1 = 0.9$ and $P_2 = 0.1$ and $\kappa = \mu = 1$

performance as depicted in the analysis performed in the earlier sections. The system model is further analyzed by studying the outage probability for the users U1 and U2 for both perfect SIC, i.e., $\beta = 0$ as shown in Fig. 5 and imperfect SIC condition with $\beta = 0.01$ as depicted in Fig. 6 for a code rate of 1 bps/Hz. It can be seen that the outage probability of the near user U2 will increase as the number of RIS elements increases, and in the case of the far user U1, it helps it to reach the asymptotic level more quickly.

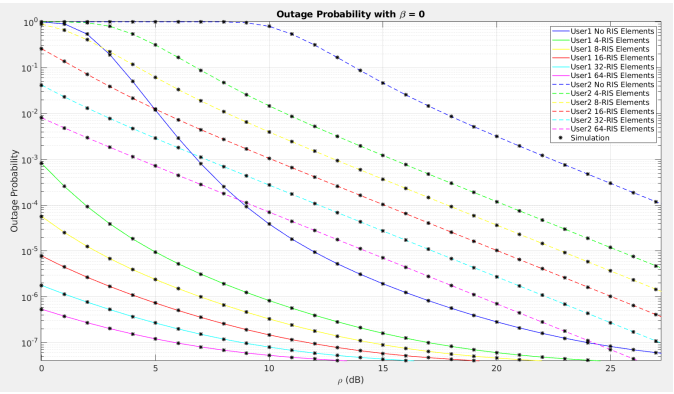

Fig. 5: Outage Probability of users U1 and U2 for various RIS scenarios with perfect SIC i.e.., $\beta = 0$ and $P_1 = 0.9$ and $P_2 = 0.1$ and $\kappa = \mu = 1$

Figs. 7 and 8 show the ergodic capacity of users U1 and U2 with power allocations $P_1 = 0.9$ and $P_2 = 0.1$ for both the perfect SIC case, i.e., $\beta = 0$, and the imperfect SIC case with $\beta = 0.01$, respectively. It is evident from the plots that the ergodic capacity of the users will increase with the increase in the number of RIS elements, thereby enabling the base station to transmit the data at a higher bit rate, fulfilling the demand for higher throughput.

It is observed that the RIS will improve wireless communication systems by intelligently reflecting and focusing the transmitted signals. When RIS elements are integrated into a NOMA system, they help to increase the SNR at

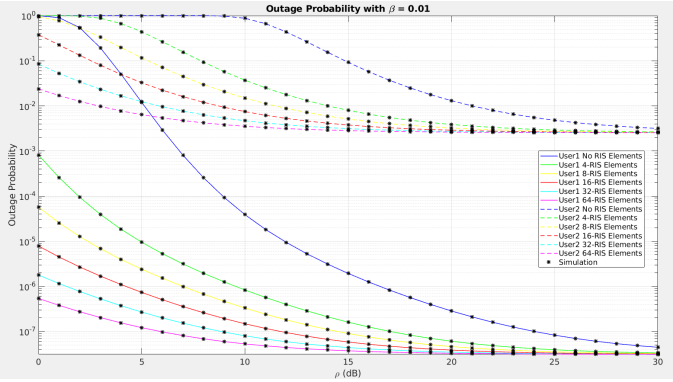

Fig. 6: Outage Probability of users U1 and U2 for various RIS scenarios with imperfect SIC i.e.., $\beta = 0.01$ and $P_1 = 0.9$ and $P_2 = 0.1$ and $\kappa = \mu = 1$

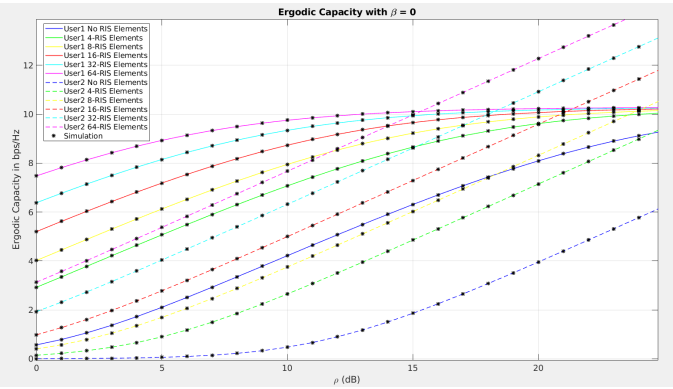

Fig. 7: Ergodic Capacity of users U1 and U2 for various RIS scenarios with perfect SIC i.e.., $\beta = 0$ and $P_1 = 0.9$ and $P_2 = 0.1$ and $\kappa = \mu = 1$

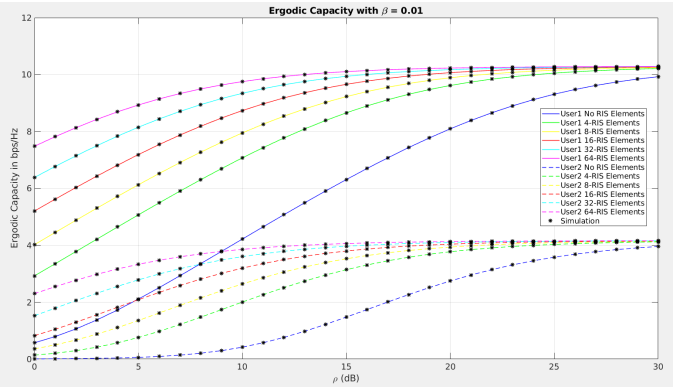

Fig. 8: Ergodic Capacity of users U1 and U2 for various RIS scenarios with imperfect SIC i.e.., $\beta = 0.01$ and $P_1 = 0.9$ and $P_2 = 0.1$ and $\kappa = \mu = 1$

the receiver by enhancing the signal quality, leading to more reliable communication. This makes the system more robust and resilient against noise and interference. Also, the far user (U1) typically suffers from higher interference than the near user (U2) because it is farther from the base station. The far user's performance is often constrained by the power allocation to the near user. Since the near user's signal is treated as interference by the far user (while decoding), the far user's achievable data rate and error performance are limited.

VII. Conclusion

This paper provides a comprehensive quantitative analysis of a two-user non-orthogonal multiple access (NOMA) system, considering scenarios with and without reconfigurable intelligent surface (RIS) elements. Key performance metrics, including Bit Error Rate (BER), outage probability, and ergodic capacity, were analyzed under the $\kappa-\mu$ fading channel model, with a focus on both perfect and imperfect Successive Interference Cancellation (SIC). The results reveal that integrating RIS elements into NOMA systems significantly enhances overall performance. Specifically, RIS elements effectively mitigate interference, improve signal quality, and boost the signal-to-noise ratio (SNR) for both near and far users. This enhancement is especially pronounced under imperfect SIC conditions, where the system's robustness becomes critical. The study also demonstrates that the performance gains are more substantial as RIS elements increase, leading to better BER, reduced outage probability, and higher ergodic capacity.

References

[1] L. Dai, B. Wang, Y. Yuan, S. Han, C.-L. I, and Z. Wang, "Non-orthogonal multiple access for 5G: solutions, challenges, opportunities, and future research trends," *IEEE Communications Magazine*, vol. 53, no. 9, pp. 74–81, 2015.

[2] K. P. Peppas, "Dual-Hop Relaying Communications with Cochannel Interference Over η–μ Fading Channels," *IEEE Transactions on Vehicular Technology*, 2013.

[3] A. Rauniyar, O. N. Østerbø, J. E. Håkegård, and P. E. Engelstad, "Ergodic Performance Analysis of Reconfigurable Intelligent Surface Enabled Bidirectional NOMA," *IEEE Transactions on Wireless Communications*.

[4] X. Yue and Y. Liu, "Performance Analysis of Intelligent Reflecting Surface Assisted NOMA Networks," *IEEE Transactions on Wireless Communications*.

[5] M. H. Kumar, S. Sharma, K. Deka, and M. Thottappan, "Reconfigurable Intelligent Surfaces Assisted Hybrid NOMA System," *IEEE Communications Letters*.

[6] G. Li, H. Liu, G. Huang, X. Li, B. Raj, and F. Kara, "Effective Capacity Analysis of Reconfigurable Intelligent Surfaces Aided NOMA Network," *Journal of Wireless Communications and Networking*.

[7] V. B. Kumaravelu, A. L. Imoize, F. R. Castillo Soria, P. G. Sivabalan, S. J. Thiruvengadam, D.-T. Do, and A. Murugadass, "RIS-Assisted Fixed NOMA: Outage Probability Analysis and Transmit Power Optimization," *Future Internet*.

[8] S. M. Awad and M. A. Hafez, "Ergodic Capacity Analysis of Downlink NOMA Systems Over Shadowed Fading Channels," *2023 IEEE Virtual Conference on Communications (VCC)*, NY, USA, 2023, pp. 241–245.

[9] A. Nosratinia, T. E. Hunter, and A. Hedayat, "Cooperative communication in wireless networks," *IEEE Communications Magazine*, vol. 42, no. 10, pp. 74–80, 2004.

[10] M. Zeng, W. Hao, O. A. Dobre, and Z. Ding, "Cooperative NOMA: State of the art, key techniques, and open challenges," *IEEE Network*, vol. 34, no. 5, pp. 205–211, 2020.

[11] L. Lv, J. Chen, and Q. Ni, "Cooperative non-orthogonal multiple access in cognitive radio," *IEEE Communications Letters*, vol. 20, no. 10, pp. 2059–2062, Oct. 2016.

[12] S. M. Awad and M. A. Hafez, "Outage performance analysis of downlink NOMA systems with imperfect SIC over κ–μ shadowed fading channels," in *2024 IEEE International Black Sea Conference on Communications and Networking (BlackSeaCom)*, Tbilisi, Georgia, 2024, pp. 304–307.